

Downregulation of PTP1B and TC-PTP phosphatases potentiate dendritic cell-based immunotherapy through IL-12/IFN γ signaling

Claudia Penafuerte^a, Matthew Feldhammer^{a,b}, John R. Mills^b, Valerie Vinette^{a,b}, Kelly A. Pike^a, Anita Hall^{a,c}, Eva Migon^a, Gerard Karsenty^d, Jerry Pelletier^{a,b}, George Zogopoulos^{a,c}, and Michel L. Tremblay^{a,b}

^aGoodman Cancer Research Centre, McGill University, Montreal, QC, Canada; ^bDepartment of Biochemistry, McGill University, Montreal, QC, Canada; ^cMcGill University Health Centre-Research Institute, MUHC-RI, Montreal, QC, Canada; ^dColumbia University, New York, NY, USA

ABSTRACT

PTP1B and TC-PTP are highly related protein-tyrosine phosphatases (PTPs) that regulate the JAK/STAT signaling cascade essential for cytokine-receptor activation in immune cells. Here, we describe a novel immunotherapy approach whereby monocyte-derived dendritic cell (moDC) function is enhanced by modulating the enzymatic activities of PTP1B and TC-PTP. To downregulate or delete the activity/expression of these PTPs, we generated mice with PTP-specific deletions in the dendritic cell compartment or used PTP1B and TC-PTP specific inhibitor. While total ablation of PTP1B or TC-PTP expression leads to tolerogenic DCs via STAT3 hyperactivation, downregulation of either phosphatase remarkably shifts the balance toward an immunogenic DC phenotype due to hyperactivation of STAT4, STAT1 and Src kinase. The resulting increase in IL-12 and IFN γ production subsequently amplifies the IL-12/STAT4/IFN γ /STAT1/IL-12 positive autocrine loop and enhances the therapeutic potential of mature moDCs in tumor-bearing mice. Furthermore, pharmacological inhibition of both PTPs improves the maturation of defective moDCs derived from pancreatic cancer (PaC) patients. Our study provides a new advance in the use of DC-based cancer immunotherapy that is complementary to current cancer therapeutics.

ARTICLE HISTORY

Received 23 January 2017
Revised 16 April 2017
Accepted 17 April 2017

KEYWORDS

Dendritic cells (DCs); immunotherapy; protein-tyrosine phosphatases; PTP1B; TC-PTP

Introduction

The Janus kinase/signal transducer and activator of transcription (JAK/STAT) signaling pathway plays a crucial role in the processes of hematopoiesis, immune cell proliferation, differentiation and immunological functions.¹ Two highly related protein-tyrosine phosphatases (PTPs), TC-PTP and PTP1B are major negative regulators of the JAK/STAT signaling cascade. These enzymes display over 75% sequence identity in their catalytic domain and overlap in some of their substrate recognition profiles. *In vitro* analysis with substrate-trapping mutants indicates that PTP1B stably interacts with JAK2 and TYK2² leading to the inhibition of STAT4 and STAT3 activation,^{3,4} whereas TC-PTP interacts with JAK1 and JAK3 leading to inhibition of STAT1, STAT3 and STAT5 activation.⁵⁻⁷


JAK/STAT signaling pathways are crucial regulators of dendritic cell (DC) differentiation, cytokine production, and DC-mediated T helper 1 (T_H1) development required for an effective antitumor response.⁸ Optimal interleukin 12 (IL-12) production constitutes the third DC-derived signal essentially required for T cell activation and differentiation into Th1 cells.⁹ IL-12 induces tyrosine phosphorylation and activation of IL-12 receptor through JAK2 and TYK2, which phosphorylates and activates STAT4. This signaling event leads to DC activation in

an autocrine manner, as well as IL-12-dependent IFN γ production by DCs.¹⁰

Previous studies have reported the activation of Src tyrosine kinases as part of the signaling cascade downstream TLR activation in DCs. As evidence, the treatment with a Src-specific inhibitor significantly affects the production of pro-inflammatory cytokines without altering the costimulatory molecule expression in DCs stimulated with TLR agonists. Consequently, DCs with impaired Src activation fail to induce efficient Th1 cell differentiation.^{11,12} Src tyrosine kinase has been identified as an interacting protein of PTP1B in myeloid DCs, in which, Src dysregulation in the absence of PTP1B is associated with low podosome numbers and focal contacts resulting in defects of migration and T cell stimulation after DC maturation stimulus.¹³

Cancer patients display a significant reduction in mature and functional DCs and have an aberrant accumulation of immature myeloid cells.^{14,15} DCs derived from cancer patients express very low levels of co-stimulatory molecules CD80 and CD86, promoting T cell tolerance or anergy.¹⁶ Thus, tumor-associated defects in DC function count as major factors responsible for tumor escape from immune surveillance.

CONTACT Michel L. Tremblay  michel.tremblay@mcgill.ca

 Supplemental data for this article can be accessed on the [publisher's website](#).

Published with license by Taylor & Francis Group, LLC © Claudia Penafuerte, Matthew Feldhammer, John R. Mills, Valerie Vinette, Kelly A. Pike, Anita Hall, Eva Migon, Gerard Karsenty, Jerry Pelletier, George Zogopoulos, and Michel L. Tremblay.

This is an Open Access article distributed under the terms of the Creative Commons Attribution-NonCommercial-NoDerivatives License (<http://creativecommons.org/licenses/by-nc-nd/4.0/>), which permits non-commercial re-use, distribution, and reproduction in any medium, provided the original work is properly cited, and is not altered, transformed, or built upon in any way.

Here, we report that differential PTP1B and TC-PTP activity influences the maturation and activation state of myeloid DCs through regulation of JAK/STAT and Src signaling. The downregulation (heterozygous, Het) of PTP1B and TC-PTP induce highly immunogenic DCs, whereas gene deletion (knockout, KO) of these PTPs gives rise to DCs with an impaired capacity for CD4⁺ T cell activation. Importantly, simultaneous downregulation of both PTPs through genetic or pharmacological means restores antigen-presentation capacity and cytokine production in defective moDCs from pancreatic cancer (PaC) patients. In conclusion, activity of these two phosphatases can alter the degree of antitumor immune response by regulating JAK/STAT and Src signaling pathways in myeloid DCs.

Results

PTP1B differential expression influence DC maturation and antitumor response

We set out to determine the contribution of PTP1B to the immune response using a B cell lymphoma transgenic mouse model (*Eμ-myc*), which mimics human Burkitt's lymphoma. We generated *Eμ-myc* mice that were PTP1B null and Het (*Eμ-myc:1B^{-/-}* and *Eμ-myc:1B^{+/-}*, respectively) by breeding the transgenic *myc* and *PTPN1* strains and monitoring tumor growth and survival overtime. *Eμ-myc:1B^{+/-}* mice displayed a significant delay in tumor development and showed increased survival compared with *Eμ-myc:1B^{-/-}* ($p = 0.0003$) and *Eμ-myc:1B^{+/+}* ($p < 0.0001$). By 80 d of age, 95% of *Eμ-myc:1B^{+/-}* mice were tumor-free compared with 65% of *Eμ-myc:1B^{-/-}* and 49% of *Eμ-myc:1B^{+/+}*. By 120 d of age, 46% of *Eμ-myc:1B^{+/-}* mice were tumor-free compared 11% of *Eμ-myc:1B^{-/-}* and 7% of *Eμ-myc:1B^{+/+}*. No significant differences in survival were observed between *Eμ-myc:1B^{-/-}* and *Eμ-myc:1B^{+/+}* in this tumor model (Fig. 1A).

To characterize the antitumor immune response in the context of *PTPN1* gene loss (PTP1B knockout) or downregulation (PTP1B heterozygous), we quantified the number of immune cell types infiltrated in the tumor site. Here, wild type (wt), PTP1B Het (*1B^{+/-}*) and PTP1B KO (*1B^{-/-}*) mice received subcutaneous injections of 10^6 *Eμ-myc* B cell lymphomas mixed in matrigel. Compared with wt and *1B^{+/-}*, the *1B^{-/-}* implants contain a significantly higher number of dendritic cells based on the expression of CD11c, whereas the number of the rest of immune cell types analyzed were similar to ones in the wt implants. In contrast, the tumor implants from *1B^{+/-}* mice display a similar number of DCs compared with the WT implants. However, we observe a decrease in the numbers of immune suppressor cells, such as: granulocyte myeloid-derived suppressor cells (G-MDSC: CD11b⁺/Gr-1⁺/Ly6G⁺) and regulatory T cells (Treg: CD4⁺/Foxp3⁺) compared with wt and *1B^{-/-}* implants (Fig. 1B).

Since we observed a significantly higher number of DCs in the implants from *1B^{-/-}* mice but a significant decrease in survival rate compared with *1B^{+/-}* mice, we investigated the maturation state of the tumor-infiltrated DCs (CD11c cells) in the three groups.

Tumor-infiltrated DCs extracted from *1B^{+/-}* mice displayed significantly higher MHC class I expression than wt DCs and

higher MHC class II expression than wt and *1B^{-/-}* DCs, which indicates a more immunogenic phenotype (Figs. 1C and D and S1). We confirmed the expression of PTP1B in the CD11c⁺ cells (DCs) isolated from these mice (Fig. 1E). These results suggest that differential PTP1B expression/activity can influence the maturation state of DCs and consequently the antitumor response *in vivo*.

We hypothesized that PTP1B downregulation would affect cytokine receptor signaling, which enhances DC maturation and activation leading to a more effective antitumor response and increased survival. To validate our hypothesis, we generated mice carrying a DC-specific deletion of PTP1B and its highly related phosphatase, TC-PTP. Mature monocyte-derived DCs (moDCs) were generated from tissue-specific PTP1B-deficient CD11c-Cre mice. Approximately 94–95% purity was achieved for both immature and mature moDCs. The efficiency of PTPN1 (PTP1B) and PTPN2 (TC-PTP) deletion in the CD11c-Cre mice was assessed by western blot with mature moDCs. As a result of these crosses, we obtained mice that were knockout and heterozygous for PTP1B (*1B^{fl/fl}* and *1B^{fl/wt}*) and TC-PTP (*TC^{fl/fl}* and *TC^{fl/wt}*) respectively only in the dendritic cell compartment (CD11c⁺ cells) (Fig. S2).

The lymphoma mouse model E.G7-OVA expressing luciferase was used as a proof of concept to specifically determine the magnitude of the antitumor response and therapeutic properties of PTP1B-deficient (*1B^{fl/wt}* and *1B^{fl/fl}*) moDCs. Mice with pre-established tumors (Fig. 2A) were treated with one intraperitoneal (IP) injection of 5×10^6 OVA-pulsed mature PTP1B-deficient moDCs or mature wt (*Cre⁻ wt/wt*) moDCs. *1B^{fl/wt}* moDC treatment in tumor-bearing mice provides a greater therapeutic benefit compared with *1B^{fl/fl}* or wt moDC treatments, based on the significant delay of tumor growth over time (Fig. 2B and C). Based on the previous results, we examined the ability of chicken ovalbumin (OVA)-pulsed PTP-deficient moDCs to activate CD8⁺ or CD4⁺ T cells derived from OT-I and OT-II transgenic mice, respectively. OVA-pulsed mature moDCs were co-cultured with CD8⁺ or CD4⁺ T cells for 48 h and IFN γ secreted as an indicator of T cell activation was quantified by ELISA. *1B^{fl/wt}* moDCs acted as significantly more potent antigen-presenting cells to CD4⁺ and CD8⁺ T cells than wt or *1B^{fl/fl}* moDCs, respectively. In contrast, *1B^{fl/fl}* moDCs displayed an impaired capacity for CD4⁺ T cell activation, (Fig. 2D). As the most relevant phenotypic feature, mature *1B^{fl/wt}* moDCs secrete higher levels of Th1-polarizing cytokines IL-12 and IFN γ than wt moDCs. *1B^{fl/fl}* moDCs produced reduced levels of IFN γ and IL-12 (Fig. 2E and F). Furthermore, matured *1B^{fl/wt}* moDCs display more immunogenic phenotype than wt moDCs characterized by higher MHC class I and CD86 expression (Fig. 2G).

The downregulation of TC-PTP, a highly related PTP1B phosphatase, similarly affects DC maturation state

As described previously, mice with pre-established tumors (Fig. 3A) were treated with one IP injection of 5×10^6 OVA-pulsed mature TC-PTP-deficient moDCs or mature wt moDCs. Eight days post-TC^{fl/wt} moDC treatment, we observed a significant delay in tumor growth compared

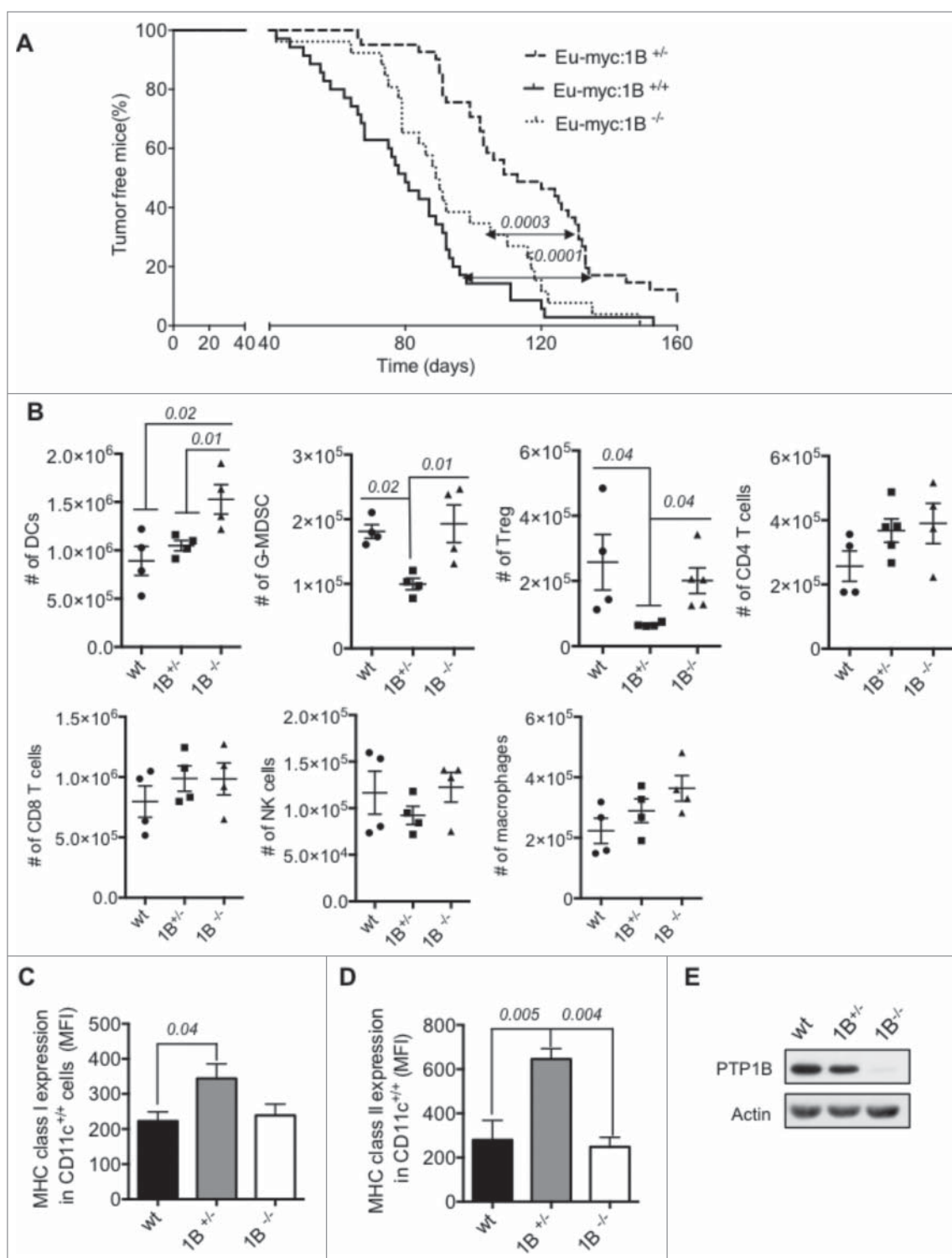


Figure 1. Effect of PTP1B phosphatase on the antitumor immune response in Eμ-myc mouse model of B cell lymphoma. (A) Tumor-free mice curve of Eμ-myc mice crossed with full body PTP1B KO (Eμ-myc:1B^{-/-}), Het (Eμ-myc:1B^{+/-}) or wt mice (*n* = 22 per group). Quantification of immune cells infiltrated at the tumor site: (B) Absolute number of immune cells infiltrated in the tumor site. DCs (CD11c⁺), granulocyte-derived myeloid suppressor cells (G-MDSC: CD11b⁺/Gr-1⁺/Ly-6G⁺), regulatory T cells (Treg: CD4⁺/FoxP3⁺), CD4⁺ T cells (CD4⁺/CD3⁺), CD8⁺ T cells (CD8⁺/CD3⁺), NK cells (NK1.1⁺/CD3⁻) and macrophages (F4/80) (*n* = 4). Expression of MHC I/II on tumor-infiltrated DCs. (C) MHC class I. (D) MHC class II (*n* = 4). (E) PTP1B expression in CD11c⁺ cells isolated from the bone marrow of Eμ-myc:1B^{-/-}, Eμ-myc:1B^{+/-} or wt mice. The results are representative of three independent experiments. The comparisons were determined using One-Way ANOVA (Holm-Sidak multiple comparison test) for parametric and Dunn's multiple test for non-parametric. *p* values are indicated.

with untreated and TC^{fl/fl} moDC treated groups of mice (Fig. 3B and C). Similarly, mature TC^{fl/wt} moDC induce greater CD4⁺ and CD8⁺ T cell activation *in vitro* and produce significant amount of IL-12 and IFNγ. TC^{fl/fl} moDCs display a

dramatic decrease in the capability for CD4⁺ T cell activation and IFNγ production in comparison with wt moDCs (Fig. 3D–F). As previously observed in mature 1B^{fl/wt} moDC, mature TC^{fl/wt} moDCs also exhibit a more immunogenic phenotype

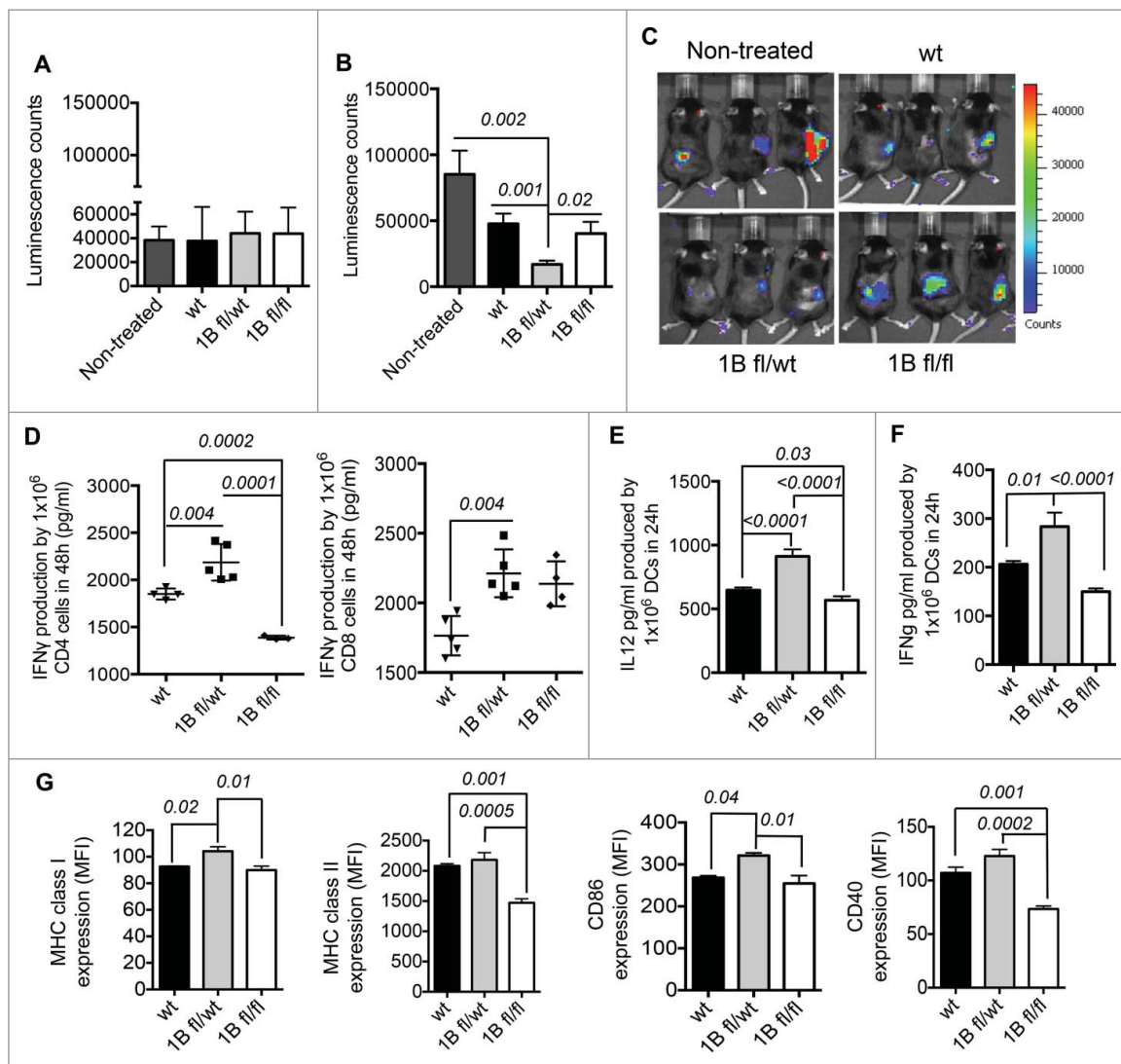


Figure 2. Characterization of PTP1B deficient moDCs. (A) Therapeutic effect of PTP1B deficient moDCs in a mouse model of lymphoma E.G7-OVA: Tumor volume before moDC treatments (10 d after implantation of 5×10^5 E.G7-OVA cells) and (B) 18 d after tumor implantation and 8 d after intraperitoneal (IP) injections of 5×10^6 1B-deficient moDCs compared with control group (tumor-bearing mice without moDC treatment). (C) *In vivo* images of tumor-bearing mice 8 d after moDCs treatments ($n = 5$). (D) Quantification of IFN γ produced by activated OT-II CD4 $^+$ T and OT-I CD8 $^+$ T cells respectively co-cultured with mature and OVA-pulsed 1B $^{fl/fl}$, 1B $^{fl/wt}$ or wt moDCs during 48 h ($n = 4-5$). The amount of IFN γ produced by mature PTP1B-deficient or wt moDCs was subtracted for both OT-II CD4 $^+$ and OT-I CD8 $^+$ co-cultures. Production of Th1 polarizing cytokines ($n = 5$): (E) IL-12 and (F) IFN γ . (G) Mean Fluorescent Intensity (MFI) values of the expression of MHC class I, MHC class II, CD86 and CD40 ($n = 3$). The comparisons were determined using One-Way ANOVA (Holm-Sidak multiple comparison test) for parametric and Dunn's multiple test for non-parametric. The results are representative of at least three independent experiments. *p* values are indicated.

based on higher MHC class I and CD86 expression than wt moDCs (Fig. 3G).

Both PTP1B and TC-PTP independently potentiate moDC functions through their substrate activation

We analyzed the activation status of PTP1B and TC-PTP substrates in the JAK/STAT signaling pathway and specifically the activation status of STAT molecules downstream of cytokine receptors in terminally differentiated and mature moDCs. STAT4 and STAT1 were significantly more phosphorylated in 1B $^{fl/wt}$ moDCs and TC $^{fl/wt}$ moDCs compared with wt moDCs, whereas STAT3 and STAT5 appeared to be hyper-phosphorylated in both 1B $^{fl/fl}$ moDCs

and TC $^{fl/fl}$ moDCs (Fig. 4A and B). We determined the activation status of the PTP1B-regulated kinase, Src, associated with TLR4.¹³ Compared with wt moDCs, both 1B $^{fl/wt}$ and TC $^{fl/wt}$ moDCs exhibit significantly increased phosphorylation of Src (Y416) that upregulates the enzyme activity, as well as higher I κ B α phosphorylation, an indicator of NF- κ B activation downstream of TLR4 engagement (Fig. 4C and D). On the other hand, we determined noticeable differences between 1B $^{fl/fl}$ moDCs and TC $^{fl/fl}$ moDCs for the Src (Y416), NF- κ B and STAT1 signaling. In 1B $^{fl/fl}$ moDCs, Src signaling is more activated than in wt DCs whereas in TC $^{fl/fl}$ moDCs, I κ B α and STAT1 are higher phosphorylated than the ones in wt DCs (Fig. 4). These results suggest that PTP1B and TC-PTP do not play redundant roles in DC functions.

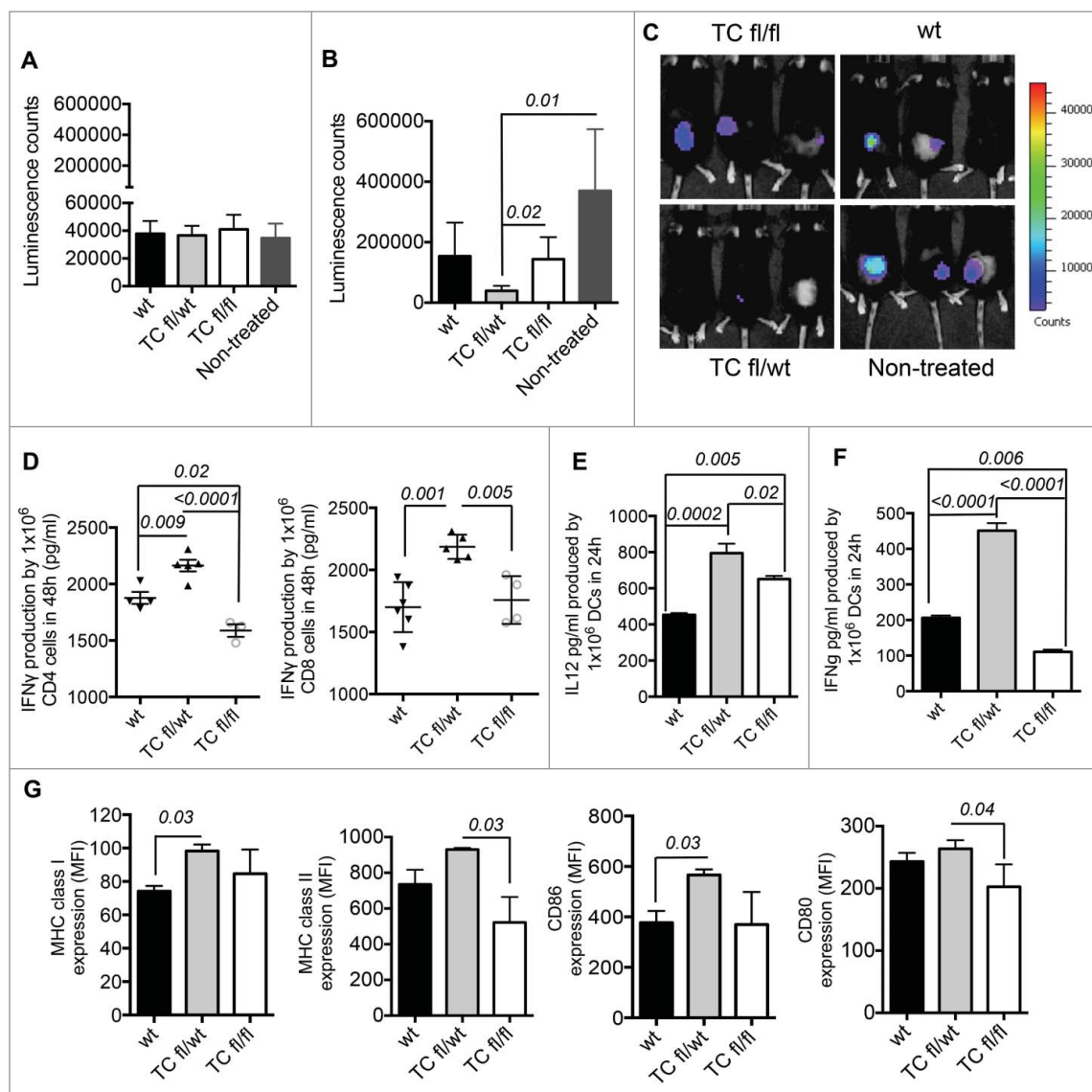


Figure 3. Characterization of TC-PTP deficient moDCs. (A) Therapeutic effect of TC-PTP deficient moDCs in a mouse model of lymphoma E.G7-OVA: Tumor volume before moDC treatment (10 d after implantation of 5×10^5 E.G7-OVA cells) and (B) after IP injections of 5×10^6 TC-deficient moDC compared with control group (tumor-bearing mice without moDC treatment). The IP injections with moDCs were given 18 d after tumor implantation. (C) *In vivo* images of tumor-bearing mice 8 d after moDC treatment. (D) Quantification of IFN γ produced by activated OT-II CD4 $^+$ T and OT-I CD8 $^+$ T cells respectively co-cultured with mature and OVA-pulsed TC $^{fl/fl}$, TC $^{fl/wt}$ or wt moDCs during 48 h ($n = 3-5$) and ($n = 6-4$). The amount of IFN γ produced by mature TC-PTP-deficient or wt moDCs was subtracted for both OT-II CD4 $^+$ and OT-I CD8 $^+$ co-cultures. Production of Th1 polarizing cytokines ($n = 5$): (E) IL-12 and (F) IFN γ . (G) MFI values of the expression of MHC class I and II, CD86 and CD80 ($n = 3$). The comparisons were determined using One-Way ANOVA (Holm-Sidak multiple comparison test) for parametric and Dunn's multiple test for non-parametric. The results are representative of three independent experiments. p values are indicated in the figures.

Simultaneous downregulation of PTP1B and TC-PTP exerts additive effect on DC functions

To investigate how contemporaneous downregulation of both PTP1B and TC-PTP affects DC functions, we generated PTP1B and TC-PTP double heterozygous CD11c Cre mice (1B:TC $^{fl/wt}$) (Fig. S3A). 1B:TC $^{fl/wt}$ moDCs exhibited an improved maturation state with significant upregulation of MHC class I, CD86 and CD80 compared with wt moDCs and the highest production of IL-12 and IFN γ (Figs. 5A–C and S3B). The additive effect due to simultaneous downregulation of both phosphatases was also noticeable with regard to more robust CD4 $^+$ and CD8 $^+$ T cell activation than the one induced by wt moDCs (Fig. 5D and E). As molecular

mechanism, 1B:TC $^{fl/wt}$ moDCs display significantly higher phosphorylation of Src (Y416) and I κ B α than wt moDCs. In comparison with single heterozygous moDCs, Src phosphorylation levels in 1B:TC $^{fl/wt}$ moDCs were intermediary between 1B $^{fl/wt}$ moDCs and TC $^{fl/wt}$ moDCs, whereas the highest levels of I κ B α phosphorylation were observed in mature 1B:TC $^{fl/wt}$ moDCs (Fig. 5F). To assess the contribution of STAT1 and STAT4 as substrates of PTP1B and TC-PTP in the regulation of DC maturation and activation, we treated PTP-deficient or wt moDCs with a STAT1 inhibitor (fludarabine) and a STAT4 inhibitor (lisofylline) during the maturation process. As expected, STAT1 and STAT4 phosphorylation levels were significantly higher in 1B $^{fl/wt}$ moDCs, TC $^{fl/wt}$ moDCs and 1B:TC $^{fl/wt}$ moDCs than

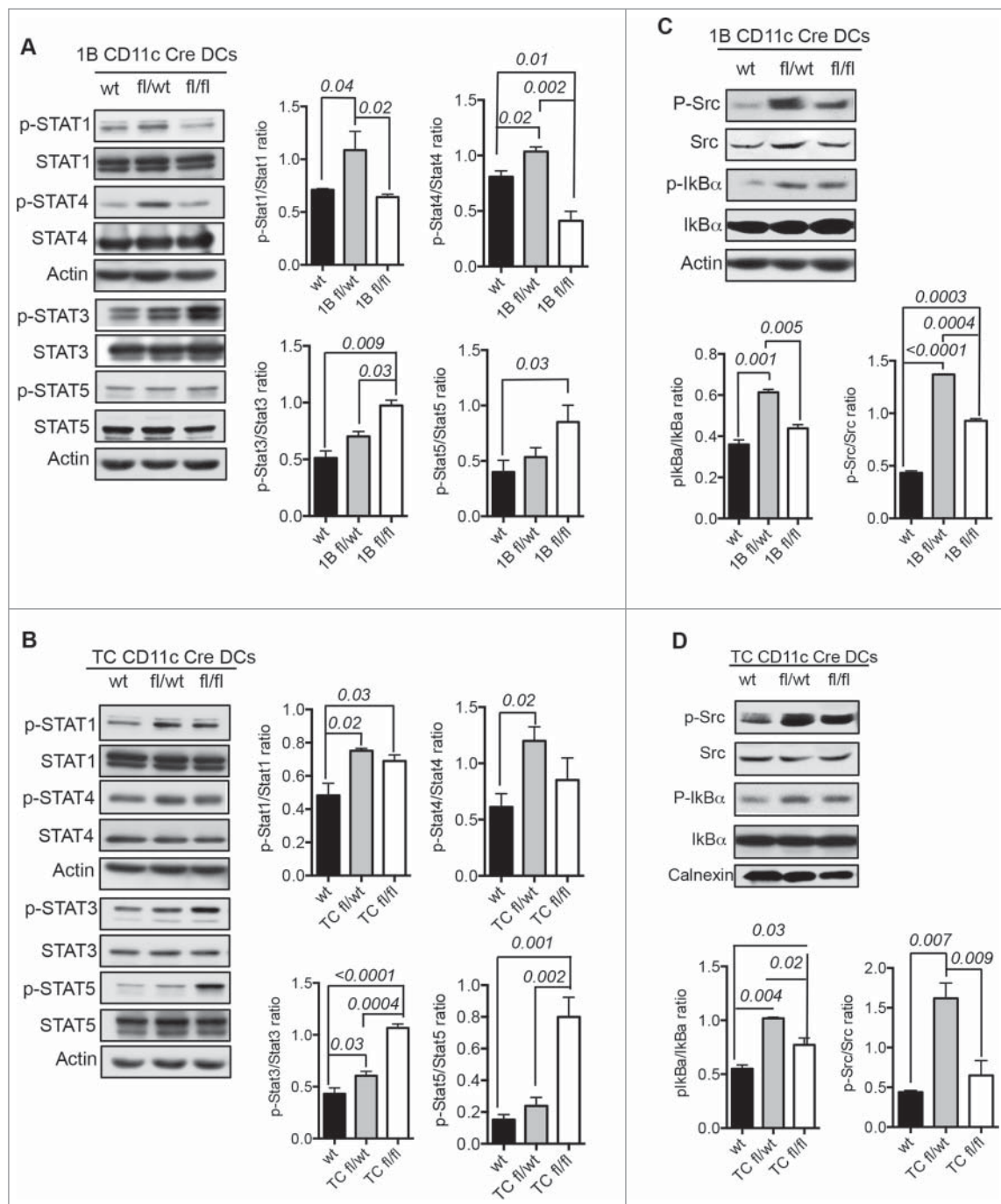


Figure 4. Molecular mechanisms of PTP1B and TC-PTP downregulation in moDCs. (A) Activation status of STAT proteins in PTP1B deficient moDCs ($n = 4$). (B) Activation status of STAT proteins in TC-PTP deficient moDCs ($n = 3$). (C) Activation status of Src kinase and $\text{IkB}\alpha$ downstream of TLR4 in PTP1B deficient moDCs ($n = 4$). (D) Activation status of Src kinase and $\text{IkB}\alpha$ in TC-PTP deficient moDCs ($n = 3$). The results are representative of three independent experiments. p values are indicated in the figures.

in wt moDCs. Both STAT1 and STAT4 specific inhibitors reciprocally affect STAT1 or STAT4 phosphorylation in $1\text{B}^{\text{fl/wt}}$ moDCs, $\text{TC}^{\text{fl/wt}}$ moDCs and $1\text{B}:\text{TC}^{\text{fl/wt}}$ moDCs, but not in the control wt moDCs, in which each STAT inhibitor specifically acts on their target molecules (STAT1 inhibitor affects STAT1 phosphorylation whereas STAT4 inhibitor impairs STAT4 phosphorylation). These results suggest a positive autocrine loop operating in moDCs deficient for these two phosphatases (Fig. 5G). Consequently, $\text{IFN}\gamma$ production, which is highly dependent on IL-12-induced STAT4 activation, not only decreased in

lisofylline-treated $\text{TC}^{\text{fl/wt}}$ moDCs, $1\text{B}^{\text{fl/wt}}$ moDCs and $1\text{B}:\text{TC}^{\text{fl/wt}}$ moDCs, but also in these cells treated with fludarabine compared with non-treated cells. IL-12 production was not affected by inhibition of STAT1 activation (fludarabine treatment) but was significantly decreased in lisofylline-treated $\text{TC}^{\text{fl/wt}}$ moDCs and $1\text{B}^{\text{fl/wt}}$ moDCs. Wild-type moDCs produced lower amounts of $\text{IFN}\gamma$ and IL-12 and this cytokine production was not affected by either fludarabine or lisofylline treatments (Fig. 5H and I).

To support potential clinical applications of these findings, the activities of these two phosphatases were also

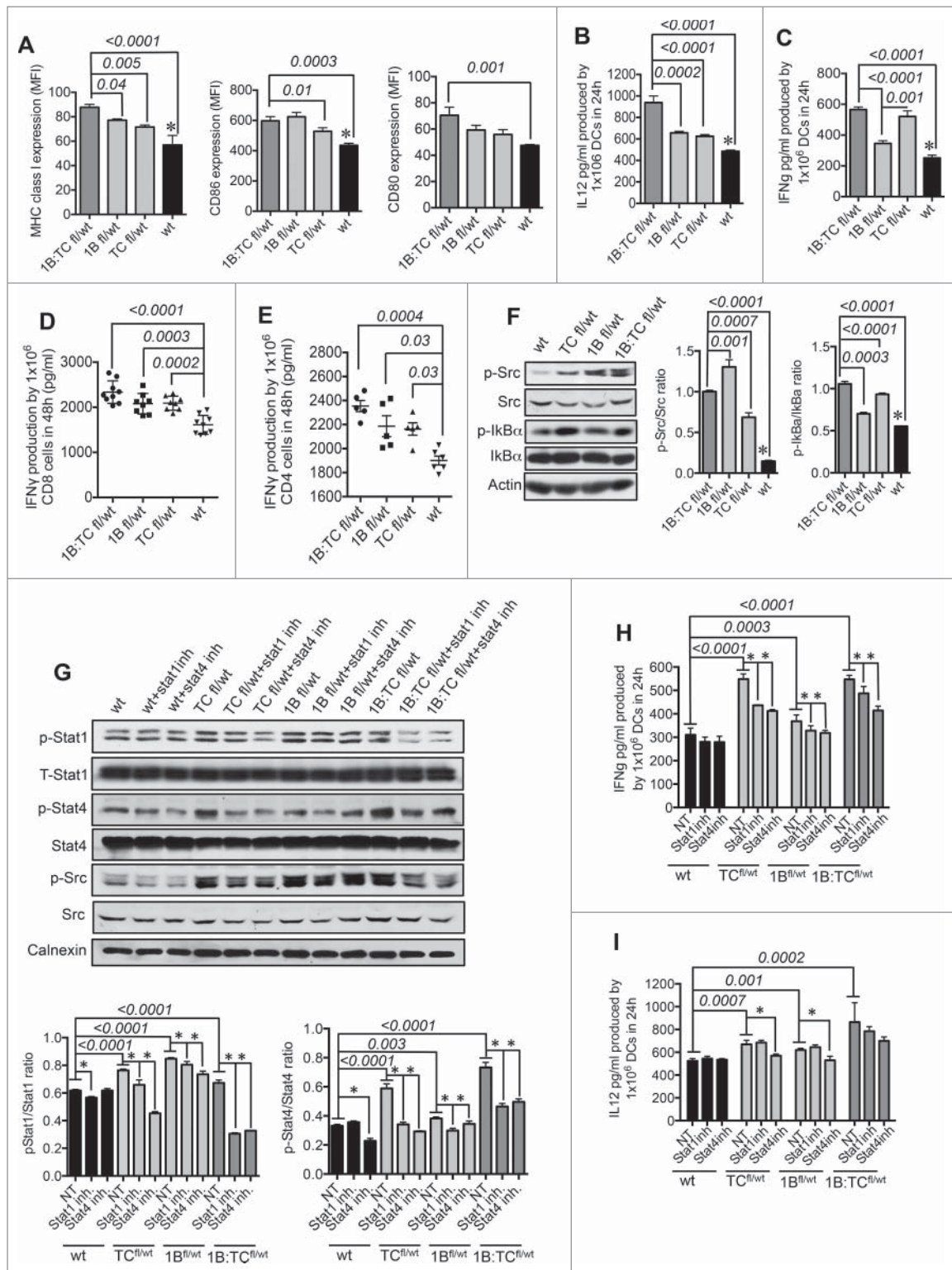


Figure 5. Simultaneous downregulation of PTP1B and TC-PTP enhances moDCs maturation. (A) Comparisons between double heterozygous (1B:TC^{fl/wt}) and TC^{fl/wt} moDCs, 1B^{fl/wt} moDCs and wt moDCs respectively. MFI values of the expression of MHC class I, CD86 and CD80 ($n = 5$). (B) Production of Th1 polarizing cytokines ($n = 5$): (B) IL-12 and (C) IFN γ . (D) Quantification of IFN γ produced by activated OT-I CD8⁺ T cells co-cultured with mature and OVA-pulsed 1B:TC^{fl/wt}, 1B^{fl/wt}, TC^{fl/wt} or wt moDCs for 48 h ($n = 8-9$). (E) Quantification of IFN γ produced by activated OT-II CD4⁺ T cells co-cultured with mature and OVA-pulsed 1B:TC^{fl/wt}, 1B^{fl/wt}, TC^{fl/wt} or wt moDCs for 48 h ($n = 5$). (F) Activation status of Src kinase and I κ B α downstream of TLR4 ($n = 3$). Significant differences are represented by p values and (*) indicate significant differences between wt DCs and the rest of the groups. (G) Activation status of STAT1, STAT4 and Src in STAT1 inhibitor (fludarabine) or STAT4 inhibitor (lisofylline) treated or non-treated 1B:TC^{fl/wt}, 1B^{fl/wt}, TC^{fl/wt} or wt moDCs ($n = 3$). Production of Th1-polarizing cytokines by 1B:TC^{fl/wt}, 1B^{fl/wt}, TC^{fl/wt} or wt moDCs previously treated with STAT1- or STAT4-inhibitor during the maturation process ($n = 3$): (H) IL-12 and (I) IFN γ . The results are representative of at least three independent experiments. Significant differences among the groups are represented by p values and (*) indicate significant differences within a group. The comparisons were determined using One-Way ANOVA (Holm-Sidak multiple comparison test) for parametric and Dunn's multiple test for non-parametric.

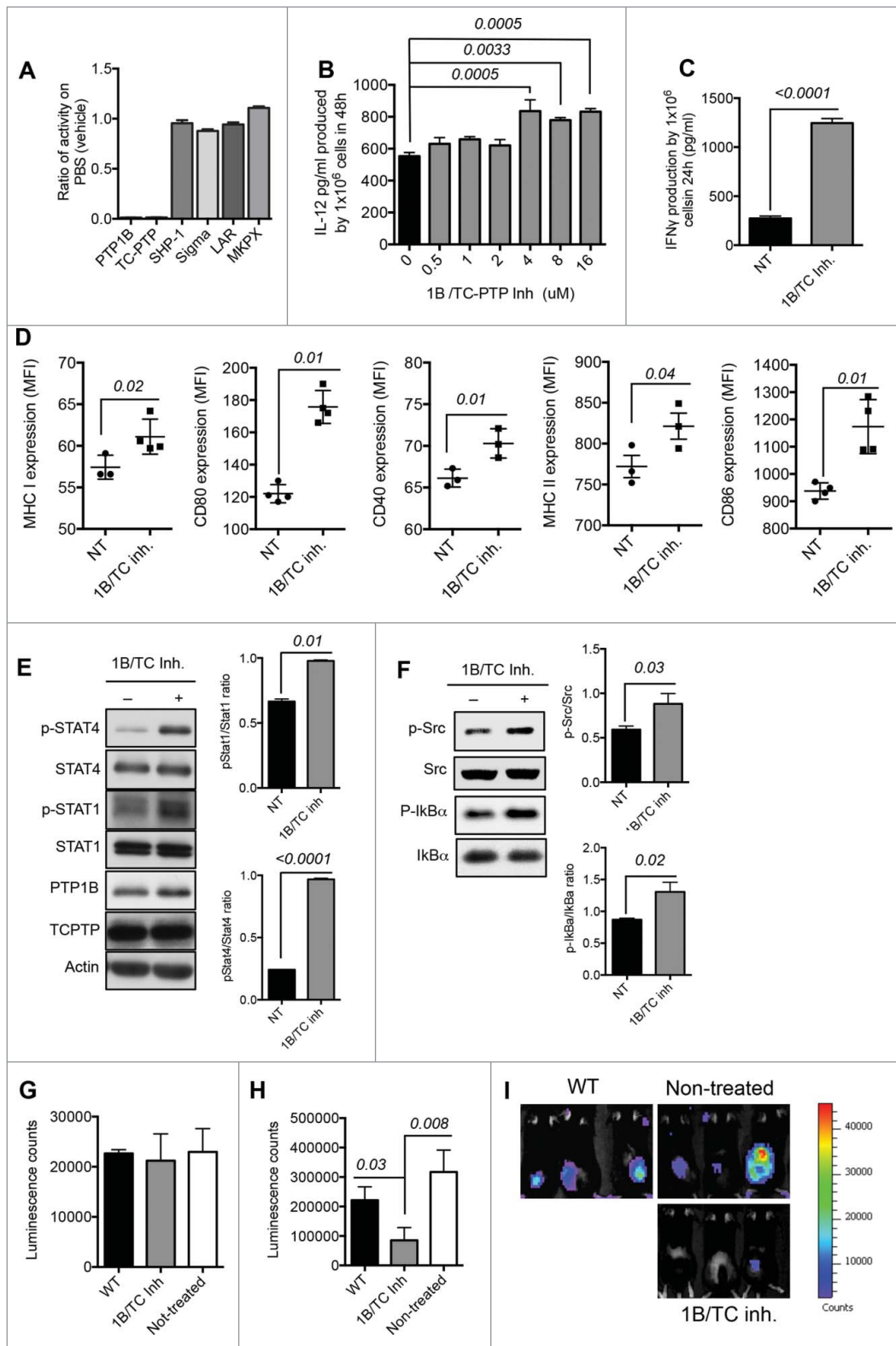


Figure 6. Pharmacological inhibition of both PTP1B and TC-PTP with specific inhibitor. (A) Specificity of 1B/TC inh (50 μ M) to inhibit PTP1B and TC-PTP dephosphorylation ($n = 3$). (B) Titration of 1B/TC inh in mouse moDCs using IL-12 production as indicator of activation ($n = 3$). (C) IFN γ production by 1B/TC inh-treated mature moDCs (4 μ M dose) ($n = 4$). (D) Expression levels (MFI) of CD40, CD80, CD86, MHC class I and II on 1B/TC inh-treated mature moDCs (4 μ M dose) ($n = 3$). (E) Activation status STAT1 and STAT4 ($n = 3$). (F) Activation status of Src kinase and I κ B α ($n = 4$). Therapeutic properties of 1B/TC inh-treated moDCs in a mouse model of E.G7 lymphoma: (G) Tumor volume before moDC treatment (10 d after implantation of 5×10^5 E.G7-OVA cells) and (H) after intraperitoneal (IP) injections of 5×10^6 1B/TC inh-treated or non-treated moDCs compared with control group (tumor-bearing mice without moDC treatments). The IP injections with moDCs were given 18 d after tumor implantation. (I) Images represent tumor-bearing mice 8 d after of moDC treatment. The results are representative of at least three independent experiments. The differences in more than two groups were determined using One-Way ANOVA (Holm-Sidak multiple comparison test) for parametric and Dunn's multiple test for non-parametric. The differences between two groups were determined with unpaired t test (two tails of distribution). Significant differences are represented by p values < 0.05 .

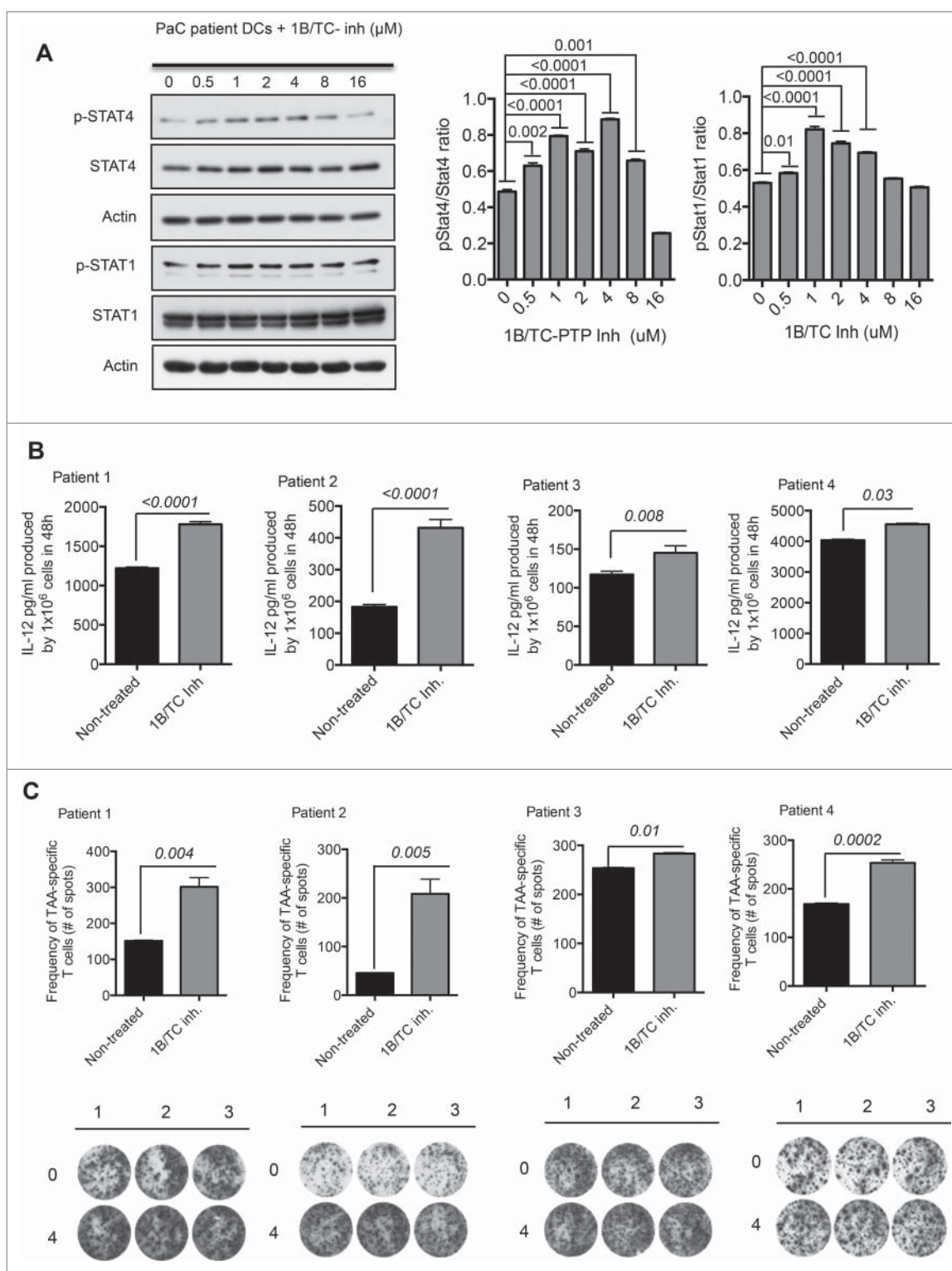


Figure 7. Application of 1B/TC inh-treated human DCs in cancer immunotherapy. (A) Activation status of STAT1 and STAT4 in 1B/TC inh-treated human moDCs derived from a pancreatic cancer (PaC) patient ($n = 3$). (B) IL-12 production by 1B/TC inh-treated human moDCs from four PaC patients. (C) Frequency of antigen-specific (CEA and CA19-9) activated T cells measured based on IFN γ production detected in ELISpot assay. The differences in more than two groups were determined using One-Way ANOVA (Holm–Sidak multiple comparison test) for parametric and Dunn’s multiple test for non-parametric. The differences between two groups were determined with unpaired t -test (two tails of distribution). Significant differences are represented by p values <0.05 .

simultaneously inhibited by pharmacological means using a specific inhibitor (1B/TC inh). The specificity of 1B/TC inh at $50 \mu\text{M}$ was determined based on the hydrolysis DiFMUP assay using different tyrosine phosphatases as controls and was found to be specific for PTP1B and TC-

PTP (Fig. 6A). In addition, a lower dose of the 1B/TC inh (0.094 – $24 \mu\text{M}$) was tested against PTP1B and TC-PTP in a hydrolysis DiFMUP assay and the inhibitory effect of 1B/TC inh was only lost at the concentrations lower than $1.5 \mu\text{M}$ (Fig. S4A).

To determine the dose at which 1B/TC inh is able to decrease PTP1B and TC-PTP activities to similar levels as the $1B^{fl/wt}$ moDCs and $TC^{fl/wt}$ moDCs, mouse monocytes were cultured in the presence of different concentrations during moDC differentiation and maturation. We did not observe any inhibitor-related cytotoxicity effect on moDCs at the highest inhibitor concentration tested ($512 \mu\text{M}$) based on the living moDC count at the end of the incubation period (Fig. S4B). IL-12 production was used as a marker of DC maturation and activation. We obtained the highest IL-12 production with a $4 \mu\text{M}$ dose of 1B/TC inh (Fig. 6B). moDCs treated with $4 \mu\text{M}$ of 1B/TC inh produced significant higher amount of $\text{IFN}\gamma$ (Fig. 6C) and exhibited greater immunogenic phenotype as characterized by increased expression of MHC class I, MHC class II, CD40, CD80 and CD86 compared with non-treated moDCs (Fig. 6D). However, 1B/TC inh treatment did not affect the cell surface expression of several chemokine receptors including CCR3, CCR5, CCR6 and CCR7 (data not shown). 1B/TC inh also induces significantly higher STAT1, STAT4, Src and I κ B α phosphorylation (Fig. 6E and F).

We investigated the therapeutic potential of 1B/TC inh-treated DCs in the mouse E.G7 lymphoma model. After 10 days, tumor-bearing mice were determined to have similar tumor burdens as measured by bioluminescence (Fig. 6G). Mice were then divided into three groups and received injections of 1B/TC inh-treated moDCs, control non-treated moDCs or no injections. Eleven days after therapeutic intervention, mice that received 1B/TC inh-treated moDCs exhibited a significant delay in tumor growth (Fig. 6H and I).

1B/TC inh restores the maturation and activation state of DCs from pancreatic cancer (PaC) patients

We investigated whether the treatment of monocytes derived from PaC patients with 1B/TC inh would enhance moDC maturation and activation. Human peripheral blood monocytes from PaC patients and healthy controls were isolated as described in the *Materials and methods* section. We obtained $3\text{--}4 \times 10^6$ human moDCs from 20–30 mL of patient blood with 98–99% purity that were CD14^- (Fig. S5A and B). 1B/TC inh was also titrated on human moDCs to define the optimal concentration to induce the highest IL-12 production (Fig. S5C). As observed in mouse moDCs, we obtained the highest activation state using a $4 \mu\text{M}$ dose, which was significantly different from non-treated DCs ($p = 0.009$). PaC-derived moDCs treated with $4 \mu\text{M}$ of 1B/TC inh displayed higher STAT1 and STAT4 phosphorylation than non-treated cells (Fig. 7A). Additionally, STAT3 activation levels decreased in the 1B/TC inh-treated human moDCs compared with non-treated cells. However, no differences in Stat3 activation were observed at the concentration range from 2 to $32 \mu\text{M}$ of the inhibitor (Fig. S5D).

The antigen-presenting properties of human 1B/TC inh-treated moDCs were assessed by $\text{IFN}\gamma$ ELISpot assays. The highly expressed PaC proteins carcinoembryonic antigen (CEA)¹⁷ and cancer antigen 19–9 (CA19–9)¹⁸ were used as TAAs, and autologous patient T cells were used as responder cells. 1B/TC inh-treated moDCs induced a higher number of

$\text{IFN}\gamma$ -producing T cells than the ones stimulated by non-treated DCs (Fig. 7B and C).

Discussion

We have shown how PTP1B activity contributes to the development of the antitumor response against B cell lymphomas in the $E\mu\text{-myc}$ mouse model. Tumors in $E\mu\text{-myc:PTP1B}^{+/-}$ mice grow with a significant delay compared with the tumor progression observed in $E\mu\text{-myc:PTP1B}^{-/-}$ and $E\mu\text{-myc:PTP1B}^{+/+}$ mice. To assess the contribution of PTP1B deficiency in the antitumor response, we quantified the number of immune cell types driven to the tumor site at 7 d post-tumor cell implantation. At this time point, the tumor's burden is extremely low. Thus, the quantity and quality of the first immune cells in the tumor site are more influenced by the effect of differential PTP expression/activity than by tumor-induced immunosuppression typically observed at high tumor burden.

In contrast to the tumor microenvironment in both $E\mu\text{-myc:PTP1B}^{-/-}$ and $E\mu\text{-myc:PTP1B}^{+/+}$ mice, $E\mu\text{-myc:PTP1B}^{+/-}$ tumors exhibit significantly lower levels of G-MDSC and Treg as well as more immunogenic DCs (based on higher MHC class I/II expression).

These results led us to investigate the effect of differential PTP1B and the highly related TC-PTP activities in the functions of DCs as major orchestrators of the immune response. With this objective, we generated mice with PTP-specific deletions in the DC compartment.

As a cell-based therapy for cancer, treatment with $TC^{fl/wt}$ moDCs or $1B^{fl/wt}$ moDCs promotes a significant delay in cancer progression in mice with pre-established tumors. The improvement in the therapeutic potential of DC-based treatment is supported by major phenotypic changes acquired as a result of PTP1B and TC-PTP down-regulation. Both $1B^{fl/wt}$ moDCs and $TC^{fl/wt}$ moDCs exhibit significantly greater expression of MHC class I, CD86 and IL-12 production, and consequently higher capacity for CD4^+ and CD8^+ T cell activation. IL-12 (IL-12p70) is the predominant cytokine for inducing the differentiation of Th1 cells that produce high amounts of $\text{IFN}\gamma$. IL-12 also blocks the activity of immune suppressor cells such as G-MDSC and M2 macrophages. In MDSC, IL-12 alters the suppressive function by downregulating the expression of ArgI and Nos (nitric oxide synthase) while promoting the upregulation of markers of DC maturation.^{19,20} In agreement with our observations, IL-12 derived from immunogenic DCs may reduce the number of MDSC in the tumor site of $1B^{fl/wt}$ mice. In contrast, $1B^{fl/fl}$ and wt tumors display an elevated number of MDSCs that act as tolerogenic antigen-presenting cells capable of promoting the expansion of antigen-specific regulatory T cells in lymphomas.²⁰

moDCs heterozygous for both PTPs exhibit hyperphosphorylation of Src, STAT4, STAT1 and NF- κ B signaling cascades. STAT1 activation in DCs is important to achieve optimal IL-12 production, IL-12 receptor expression and promotes the upregulation of co-stimulatory and MHC molecules during the maturation process. $STAT1^{-/-}$ DCs exhibit impaired upregulation of CD40, CD80, CD86 and MHC class II and consequently

reduce antigen-presentation capacity and T cell priming.²¹ STAT4 is essential for IFN γ production, as well as for the autocrine activation of DCs by IL-12 signaling.²² In turn, IFN γ induces IL-12 production via STAT1, creating a positive feedback loop that sustains the production of these two Th1-polarizing cytokines.^{21,23} On the other hand, Src activation regulates important features associated with DC maturation such as pro-inflammatory cytokine production and Th1 cell differentiation.¹²

In contrast, mature 1B^{fl/fl} and TC^{fl/fl} moDCs share phenotypic characteristics of tolerogenic DCs, the most noticeable being a significant decrease in MHC class II expression and consequently an impaired ability for CD4⁺ T cell activation. Depletion of both PTP1B and TC-PTP in moDCs leads to hyperactivation of STAT5 and STAT3 in moDCs. Although TC^{fl/fl} moDCs also display higher STAT1 phosphorylation than wt DCs, STAT3 hyperactivation overcomes STAT1-mediated effects as essential signal transducer for DC maturation. In accordance with previous reports, simultaneous DC treatment with IL-10 (inducer of STAT3 phosphorylation) and IFN γ (inducer of STAT1 phosphorylation) promotes significant increase of iNOS (inducible nitric oxide synthase) and IDO (indoleamine 2,3-dioxygenase) production by bone marrow-derived DCs and consequently an impaired DC ability to activate CD4⁺ T cells.²⁴

In line with previous studies, STAT3 hyperactivation was associated with impaired DC maturation characterized by low MHC class II and CD40 expression, along with significant reduction of IL-12.^{13,25} STAT3 activation is induced by most of the tumor-derived factors to promote abnormal DC differentiation and maturation.²⁶ Activated STAT3 decreases intracellular major histocompatibility complex II (MHCII) α/β dimers, and H2-DM levels in DCs by increasing cathepsin S activity²⁷ and affects NF- κ B recruitment to the IL-12p40 promoter,²⁸ leading to a build-up of functionally impaired and immature myeloid cells with a high immunosuppressive potential.

Simultaneous downregulation of both PTP1B and TC-PTP in moDCs by genetic (double het 1B:TC^{fl/wt} moDCs) or pharmacological approaches (1B/TC inh) gives rise to a highly immunogenic DC phenotype. The use of specific inhibitors for STAT1 and STAT4 activation in 1B^{fl/wt}, TC^{fl/wt} and 1B:TC^{fl/wt} moDCs but not in wt moDCs impairs the phosphorylation of both STAT1 and STAT4, which indicate the present of a positive feedback mechanism that operates in single and double heterozygous moDCs for these PTPs but not in wt moDCs. Consequently, treatment with either fludarabine or lisofylline interrupts the positive activation loop and impairs the production of IFN γ by 1B^{fl/wt} moDCs, TC^{fl/wt} moDCs and 1B:TC^{fl/wt} moDCs, whereas IFN γ production by wt moDCs is not affected. On the other hand, IL-12 production that mainly relies on NF- κ B activation downstream of TLR4²⁹ and IFN γ induced by IL-12-dependent STAT4 activation was only affected by STAT4 inhibition in 1B^{fl/wt} moDCs and TC^{fl/wt} moDCs, but not in 1B:TC^{fl/wt} moDCs which suggest that this positive feedback mechanism of DC activation is more amplified in the double heterozygous moDCs due to the downregulation of both PTPs.

The inhibition of both phosphatases by pharmacological means was a more effective way to achieve an optimal DC

maturation and activation since it is possible to titrate the inhibitor concentration to fine-tune both phosphatase activities. With the inhibitor, we were able not only to recapitulate the phenotype of the double het but also we observed additional upregulation of MHC class II and CD40 expression.

This is clinically relevant since patient moDCs can be activated *ex vivo* to improve DC function and subsequently provide antitumor responses once the cells are re-introduced to the patient. In conclusion, these phosphatases target the IL-12/IFN γ axis in moDCs and downregulation of their activities potentiates antitumor immune responses.

Our results indicate that it is possible to restore and enhance the maturation and activation of dysfunctional DCs derived from PaC patients by modulating the activity of PTP1B and TC-PTP. Consequently, moDCs with reduced PTP1B and TC-PTP activities will act as more effective APCs to induce potent antigen-specific T cell activation and antitumor responses for cancer immunotherapy. These studies provide considerable insight into the signaling pathways that govern the maturation and activation of DCs. Our findings may lead to a new generation of DC-based vaccines that would be complementary to existing immunotherapies.

Materials and methods

Mice

All animal procedures were performed using 6–10 week old male C57Bl/6n mice according to the Canadian Council on Animal Care ethical regulations and were approved by the McGill University Research and Ethics Animal committee. E μ -myc mice were kindly supplied by Dr. Jerry Pelletier and crossed with *Ptpn1*^{fl/fl} mice that were obtained from the laboratory of Dr. Gerard Karsenty.³⁰ Mice with the floxed *Ptpn2* allele were generated in our laboratory.⁴⁰ Mice with PTP-specific deletions in the dendritic cell compartment were obtained by crossing *Ptpn1*^{fl/fl} or *Ptpn2*^{fl/fl} mice with CD11c-Cre transgenic mice purchased from Jackson Laboratory. OT-I (C57BL/6-Tg (Tcr α Tcr β) 1100Mjb/J, stock #003831) and OT-II (B6.Cg-Tg (Tcr α Tcr β) 425Cbn/J, stock#004194) transgenic mice were purchased from The Jackson Laboratory.

Generation of murine and human DCs: Murine moDCs

Murine monocytes were isolated from the bone marrow of tissue-specific PTP-deficient mice or corresponding wt littermates by CD11b⁺ selection using the EasySep[®] mouse monocyte CD11b⁺ selection kit (StemCell Technologies, cat# 18770). Mouse monocytes were cultured with GM-CSF and IL-4 (40 ng/mL each one) (Peprotech, cat# 315–03 and 214–14 respectively) for 6 d to allow their differentiation into immature moDCs. On day 6, immature moDCs were stimulated with 1 μ g/mL LPS (Sigma, cat# L2630) for an additional 24 h to induce maturation. LPS was used as TLR4 ligand to generate immunogenic moDCs. For antigen-presentation assays, immature moDCs were pulsed with chicken ovalbumin (OVA) as the tumor-associated antigens (TAAs) and LPS and co-cultured with OT-I and OT-II T cells for 48 hours. Both supernatants and cells were collected after the incubation period. For the

generation of 1B/TC-inhibitor treated DCs, 1B/TC inh was added in the culture media during the processes of differentiation and maturation of moDCs. 1B/TC inh was kindly provided by Dr. Brian Kennedy, Merck Frosst, Pointe-Claire, QC). The originally report of this compound was made by Merck-Frosst, Inc. in a paper by Montalibet et al.³¹ Named difluoromethyl phosphonate (DFMP) inhibitor 7-bromo-6-phosphono (difluoro-methyl)-3-naphthalenitrile (PTPi), it is used to inhibit PTP1B and TC-PTP at the concentration used in this manuscript. This inhibitor was also used in previous manuscripts from the laboratory, by Julien et al.³² and more recently by Pike et al.⁴

Human moDCs

To obtain human moDCs, blood samples were obtained from advanced stage PaC patients after providing written informed consent (Dr. George Zogopoulos, McGill University Health Centre). Patient moDCs were generated from peripheral blood monocytes isolated by positive selection of CD14⁺ cells (Stem-Cell Technologies, Inc., cat# 18058). Human monocytes were cultured in monocyte attachment media for 1 h. After 1 h, the media was replaced with DC differentiation (StemXVivo serum-free DC base media, cat# CCM003) supplemented with GM-CSF (50 ng/mL, cat# 300-03) and IL-4 (35 ng/mL, cat# 200-04) and 1B/TC inh. Monocytes were cultured for 6 d in the differentiation media. On day 3, half the volume of the differentiation media was replaced with new media and cytokines. On the day 6, the media was replaced with maturation media containing monophosphoryl lipid A (MPLA-SM, 2 μg/mL, InvivoGen, cat# vac-mpla),³³ IFN γ (1000 U/mL, PeproTech, cat# 315-05) and 1B/TC inhibitor (4 μM).

Immune cell infiltration in the tumor site

To analyze the immune cell types infiltrated in the tumor site, 1×10^6 E μ -myc B cell lymphoma cells expressing green fluorescence protein (GFP) were mixed with 500 μL Matrigel (BD Biosciences, cat# 354234) at 4 °C and injected subcutaneously in PTP1B^{-/-}, PTP1B^{+/-} or wt mice. All the implants were surgically removed 7 d after implantation and enzymatically dissociated with 1.6 mg/mL of collagenase type IV (Sigma-Aldrich, cat#M9445) in PBS as previously reported.³⁴ Infiltrated cells were collected and incubated with anti-FcR III/II antibodies for 30 min and with specific cell type or isotypic control antibodies for 1 h at 4 °C. The expression of surface markers was determined by flow cytometry.

Western blot analysis

For western blot analyses, mature moDCs were lysed in radioimmunoprecipitation assay buffer. Protein samples were resolved on 10% sodium dodecyl sulfate-polyacrylamide gel electrophoresis (SDS-PAGE) and subjected to immunoblotting. The following proteins were detected using antibodies from Cell Signaling Technologies (CST) phospho-specific and total STAT1 (total-stat1 CST cat# 9172 and phospho-stat1 CST cat# 9134), STAT3 (total-stat3 CST cat# 9139 and phospho-stat3 CST cat# 9145), STAT5

(total-stat5 CST cat# 9310 and phospho-stat5 CST cat# 9356), STAT4 (total-stat4 CST cat# 2653 and phospho-stat4 CST cat# 5267), Src (total-Src CST cat# 2109 and phospho-Src CST cat# 2101), IκBα (total-IκBα CST #4812 and phospho-IκBα CST #2859), ERK (total-ERK CST cat# 9102 and phospho-ERK CST cat# 9106, p38 (total-p38 CST #9212 and phospho-p38 CST cat# 9211) and c-Jun (total-cJun CST cat# 9165 and phospho-cJun CST cat# 9261) proteins were detected using polyclonal antibodies (Cell Signaling Technology). β-Actin and Calnexin (a gift from Dr. John J.M. Bergeron) were used as a loading control and PTP1B or TC-PTP was detected with a monoclonal antibody (BD Biosciences cat# 610140 and Calbiochem cat# PH03L). Primary antibodies were followed by horseradish peroxidase-conjugated goat anti-rabbit or mouse IgG (Jackson Immuno Research Laboratories cat# 111-035-003 and cat# 115-035-062). Blots were revealed using Western lighting chemiluminescent substrate (PerkinElmer cat# NEL105001EA). The density of the bands was quantified with ImageJ software.

STAT1 and STAT4 inhibition

Mouse PTP-deficient moDCs were generated as described previously and maturation was induced for additional 24 h in the presence of LPS and 50 μM of STAT1 inhibitor (Fludarabine, R&D Systems, cat# 3495)³⁵ or 50 μM of STAT4 inhibitor (Lisofyllin, Santa Cruz Biotechnology, cat# sc-201055).³⁶ Mature moDCs were collected for western blot analysis with specific antibodies for phosphorylated and full length STAT1, STAT4 and Src.

Generation of a stable luciferase expressing lymphoma cell line

EG7-OVA lymphoma cells (ATCC) were placed in culture and subsequently infected, as described,³⁷ with a murine stem cell virus (MSCV) based IRES-GFP vector (Addgene #19360), subcloned with a firefly luciferase gene (Addgene #18751) into the multi-cloning site using BglII and XhoI restriction sites. GFP-positive lymphomas were isolated using fluorescence activated cell sorting (FACS) (BD FACSAria sorter). Pure populations of GFP-luciferase expressing cells were expanded after sorting and frozen until needed.

In vivo studies

For the tumor implantation, 5×10^5 GFP-luciferase expressing lymphoma cells were suspended in 100 μL PBS and subcutaneously injected into syngeneic C57Bl/6n 6–10 week old males. Intraperitoneal injections of mature and OVA-pulsed moDCs derived from tissue-specific PTP-deficient mice or wt moDCs were performed as indicated in the figure legends. Mice were then monitored for lymphoma development by whole body luminescence imaging (as indicated) using an IVIS 100 *in vivo* imaging system (PerkinElmer).

Phenotypic analysis of moDCs

Mature moDC cell culture supernatants were tested for the levels of IL-12 (mouse IL-12 ELISA cat# 433607 and human IL-12 cat# 431704) and IFN γ (mouse IFN γ ELISA cat# 430804 and human IFN γ cat# 430104) using enzyme-linked immunosorbent assay (ELISA) kits (BioLegend). Mature DCs were stained immediately for flow cytometry. moDC differentiation and maturation was determined via labeling with fluorescence-conjugated antibodies specific for MHC class I (cat# 311403) and class II (cat# 361706), CD80 (cat# 305219), CD252 (cat# 326307), CD40 (cat# 334309), CD86 (cat# 305421), CD83 (cat# 305305), CCR7 (cat# 353203), CCR5 (cat# 313707), CCR6 (cat# 353415), CCR3 (cat# 310707) and CD205 (cat# 342203) (BioLegend). The expression of these cell surface markers was determined by flow cytometry and analyzed using FlowJo software (TreeStar).

PTP inhibitor specificity assay

The hydrolysis of DiFMUP as a substrate for the indicated PTPs was conducted in black 96-well plates (Corning) in a final volume of 100 μ L at 25 $^{\circ}$ C essentially as described.³¹ The reaction was monitored by measuring the excitation/emission (358/450 nm) using a Varioskan plate reader (Thermo Electron). The enzyme concentration was determined by choosing a reaction rate comprised in a fluorescence range of 5–20 FU/min and reaction was conducted at the specific Km for each enzyme against DiFMUP. Km was previously determined from rates at various substrate concentrations using Michaelis–Menten equation. For the kinetic assay, the fluorescence was monitored over 10 min in 30 sec intervals and rates were calculated using a non-linear least-square fitting procedure. The 1B/TC inhibitor was diluted in PBS and reaction was performed at a final concentration of 50 μ M. PBS was used as control (vehicle) and to determine the ratio of phosphatase activity to DiFMUP in presence or not of inhibitor.

ELISpot assays

ELISpot assay for the detection of human activated antigen-specific T cells was performed as described previously,^{38,39} and according to the manufacturer's specifications (R&D Systems, cat# EL285). Briefly, patient moDCs cultured in the presence or absence of 1B/TC inh (4 μ M) were pulsed with tumor antigens CEA (BioMart cat# CDA008) and CA19–9 (LEE Biosolutions cat# 151–99) during the maturation. The pool of antigen-specific T cells was enriched by culturing total PBMC with CEA and CA19–9 proteins during 5 d in media without serum. Mature, inhibitor-treated moDCs were then co-cultured with autologous patient T cells previously isolated using CD3⁺ magnetic bead selection (StemCell Technologies, cat# 17851). DCs and T cells were co-cultured in a 2:1 ratio (5 \times 10⁵ T cells: 2.5 \times 10⁵ DCs) for 48 h. The frequency of IFN- γ producing T cells was quantified using an ELISpot plate reader (BD Biosciences).

Statistics

The differences in tumor growth over time among the groups were analyzed using Log-rank (Mantel–Cox) Chi Square test.

The differences in more than two groups were determined using One-Way ANOVA (Holm–Sidak multiple comparison test) for parametric and Dunn's multiple test for non-parametric. The differences between two groups were determined with an unpaired *t*-test (two tails of distribution). Shapiro–Wilk normality test was applied to define parametric versus non-parametric values. The statistical analyses were performed using Prism 6 (Graph-Pad Software) and *p* values < 0.05 were considered significant.

Disclosure of potential conflicts of interest

No potential conflicts of interest were disclosed.

Acknowledgments

The authors are grateful to Noriko Uetani for artwork, Cameron Black and Teri Hatzihristidis for critical reviews of the manuscript. C.P. is a recipient of a Canadian Institute of Health Research (CIHR) post-doctoral research award, M.F. is a recipient of a doctoral research studentship from CIHR, J. P. is a holder of a James McGill Chair Professor Award, G.Z. is a Clinician Scientist Scholar of the Fonds de recherche du Québec – Santé (FRQS), M. L.T. is the holder of the Jeanne and Jean-Louis Lévesque Chair in Cancer Research.

Funding

This work was supported in parts by grants from the National Institutes of Health to G.K., a Canadian Institutes of Health Research operating award (CIHR FDN-148366) to J. Pelletier, and by the following operating grants from the Rob Lutterman- CRS research program, “the ACLON-Strauss Foundation,” the Canadian Cancer Society Innovation award program, a Canadian Institutes of Health Research operating award (MOP-62887) and a CIHR Targeting High Fatality Cancers - Innovation Grant (MOP-361853) to M.L.T.

References

- Li HS, Watowich SS. Innate immune regulation by STAT-mediated transcriptional mechanisms. *Immunol Rev* 2014; 261:84-101; PMID:25123278; <https://doi.org/10.1111/imir.12198>
- Myers MP, Andersen JN, Cheng A, Tremblay ML, Horvath CM, Parisien JP, Salmeen A, Barford D, Tonks NK. TYK2 and JAK2 are substrates of protein-tyrosine phosphatase 1B. *J Biol Chem* 2001; 276:47771-4; PMID:11694501; <https://doi.org/10.1074/jbc.M009472200>
- Kissick HT, Sanda MG, Dunn LK, Pellegrini KL, On ST, Noel JK, Arredouani MS. Androgens alter T-cell immunity by inhibiting T-helper 1 differentiation. *Proc Natl Acad Sci USA* 2014; 111:9887-92; PMID:24958858; <https://doi.org/10.1073/pnas.1402468111>
- Pike KA, Hutchins AP, Vinette V, Théberge JF, Sabbagh L, Tremblay ML, Miranda-Saavedra D. Protein tyrosine phosphatase 1B is a regulator of the interleukin-10-induced transcriptional program in macrophages. *Sci Signal* 2014; 7:ra43; PMID:24803538; <https://doi.org/10.1126/scisignal.2005020>
- Simoncic PD, Lee-Loy A, Barber DL, Tremblay ML, McGlade CJ. The T cell protein tyrosine phosphatase is a negative regulator of Janus family kinases 1 and 3. *Curr Biol* 2002; 12:446-53; PMID:11909529; [https://doi.org/10.1016/S0960-9822\(02\)00697-8](https://doi.org/10.1016/S0960-9822(02)00697-8)
- Pike KA, Tremblay ML. Regulating naive and memory CD8 T cell homeostasis – a role for protein tyrosine phosphatases. *FEBS J* 2013; 280:432-44; PMID:22458809; <https://doi.org/10.1111/j.1742-4658.2012.08587.x>
- Scharl M, Hruz P, McCole DF. Protein tyrosine phosphatase non-receptor Type 2 regulates IFN-gamma-induced cytokine signaling in THP-1 monocytes. *Inflamm Bowel Dis* 2010; 16:2055-64; PMID:20848498; <https://doi.org/10.1002/ibd.21325>

8. Li HS, Watowich SS. Diversification of dendritic cell subsets: emerging roles for STAT proteins. *JAKSTAT* 2013; 2:e25112; PMID:24416644; <https://doi.org/10.4161/jkst.25112>
9. Lutz MB. Induction of CD4(+) Regulatory and polarized effector/helper T cells by dendritic cells. *Immune Netw* 2016; 16:13-25; PMID:26937228; <https://doi.org/10.4110/in.2016.16.1.13>
10. Tokumasa N, Suto A, Kagami S, Furuta S, Hirose K, Watanabe N, Saito Y, Shimoda K, Iwamoto I, Nakajima H. Expression of Tyk2 in dendritic cells is required for IL-12, IL-23, and IFN-gamma production and the induction of Th1 cell differentiation. *Blood* 2007; 110:553-60; PMID:17395783; <https://doi.org/10.1182/blood-2006-11-059246>
11. Napolitani G, Bortoletto N, Racioppi L, Lanzavecchia A, D'Oro U. Activation of src-family tyrosine kinases by LPS regulates cytokine production in dendritic cells by controlling AP-1 formation. *Eur J Immunol* 2003; 33:2832-41; PMID:14515267; <https://doi.org/10.1002/eji.200324073>
12. Kuka M, Baronio R, Valentini S, Monaci E, Muzzi A, Aprea S, De Gregorio E, D'Oro U. Src kinases are required for a balanced production of IL-12/IL-23 in human dendritic cells activated by Toll-like receptor agonists. *PLoS One* 2010; 5:e11491; PMID:20634889; <https://doi.org/10.1371/journal.pone.0011491>
13. Martin-Granados C, Prescott AR, Le Sommer S, Klaska IP, Yu T, Muckersie E, Giuraniuc CV, Grant L, Delibegovic M, Forrester JV. A key role for PTP1B in dendritic cell maturation, migration, and T cell activation. *J Mol Cell Biol* 2015; 7:517-28; PMID:26063615; <https://doi.org/10.1093/jmcb/mjv032>
14. Gabrilovich D. Mechanisms and functional significance of tumor-induced dendritic-cell defects. *Nat Rev Immunol* 2004; 4:941-52; PMID:15573129; <https://doi.org/10.1038/nri1498>
15. Almand B, Resser JR, Lindman B, Nadaf S, Clark JI, Kwon ED, Carbone DP, Gabrilovich DI. Clinical significance of defective dendritic cell differentiation in cancer. *Clin Cancer Res* 2000; 6:1755-66; PMID:10815894
16. Whiteside TL. Inhibiting the inhibitors: evaluating agents targeting cancer immunosuppression. *Expert Opin Biol Ther* 2010; 10:1019-35; PMID:20415597; <https://doi.org/10.1517/14712598.2010.482207>
17. Koide S, Homma S, Takahara A, Namiki Y, Tsukinaga S, Mitobe J, Odahara S, Yukawa T, Matsudaira H, Nagatsuma K et al. Current immunotherapeutic approaches in pancreatic cancer. *Clin Dev Immunol* 2011; 2011:267539; PMID:21922022; <https://doi.org/10.1155/2011/267539>
18. Ballehaninna UK, Chamberlain RS. The clinical utility of serum CA 19-9 in the diagnosis, prognosis and management of pancreatic adenocarcinoma: an evidence based appraisal. *J Gastrointest Oncol* 2012; 3:105-19; PMID:22811878; <https://doi.org/10.3978/j.issn.2078-6891.2011.021>
19. Steding CE, Wu ST, Zhang Y, Jeng MH, Elzey BD, Kao C. The role of interleukin-12 on modulating myeloid-derived suppressor cells, increasing overall survival and reducing metastasis. *Immunology* 2011; 133:221-38; PMID:21453419; <https://doi.org/10.1111/j.1365-2567.2011.03429.x>
20. Serafini P, Mgebhoff S, Noonan K, Borrello I. Myeloid-derived suppressor cells promote cross-tolerance in B-cell lymphoma by expanding regulatory T cells. *Cancer Res* 2008; 68:5439-49; PMID:18593947; <https://doi.org/10.1158/0008-5472.CAN-07-6621>
21. Johnson LM, Scott P. STAT1 expression in dendritic cells, but not T cells, is required for immunity to *Leishmania major*. *J Immunol* 2007; 178:7259-66; <https://doi.org/10.4049/jimmunol.178.11.7259>
22. Chiang PH, Wang L, Bonham CA, Liang X, Fung JJ, Lu L, Qian S. Mechanistic insights into impaired dendritic cell function by rapamycin: inhibition of Jak2/Stat4 signaling pathway. *J Immunol* 2004; 172:1355-63; <https://doi.org/10.4049/jimmunol.172.3.1355>
23. Conzelmann M, Wagner AH, Hildebrandt A, Rodionova E, Hess M, Zota A, Giese T, Falk CS, Ho AD, Dreger P et al. IFN-gamma activated JAK1 shifts CD40-induced cytokine profiles in human antigen-presenting cells toward high IL-12p70 and low IL-10 production. *Biochem Pharmacol* 2010; 80:2074-86; PMID:20709027; <https://doi.org/10.1016/j.bcp.2010.07.040>
24. Yanagawa Y, Iwabuchi K, Onoe K. Co-operative action of interleukin-10 and interferon-gamma to regulate dendritic cell functions. *Immunology* 2009; 127:345-53; PMID:19191915; <https://doi.org/10.1111/j.1365-2567.2008.02986.x>
25. Kortylewski M, Xin H, Kujawski M, Lee H, Liu Y, Harris T, Drake C, Pardoll D, Yu H. Regulation of the IL-23 and IL-12 balance by Stat3 signaling in the tumor microenvironment. *Cancer Cell* 2009; 15:114-23; PMID:19185846; <https://doi.org/10.1016/j.ccr.2008.12.018>
26. Nefedova Y, Huang M, Kusmartsev S, Bhattacharya R, Cheng P, Salup R, Jove R, Gabrilovich D. Hyperactivation of STAT3 is involved in abnormal differentiation of dendritic cells in cancer. *J Immunol* 2004; 172:464-74; <https://doi.org/10.4049/jimmunol.172.1.464>
27. Kitamura H, Kamon H, Sawa S, Park SJ, Katunuma N, Ishihara K, Murakami M, Hirano T. IL-6-STAT3 controls intracellular MHC class II alpha dimer level through cathepsin S activity in dendritic cells. *Immunity* 2005; 23:491-502; PMID:16286017; <https://doi.org/10.1016/j.immuni.2005.09.010>
28. Hoentjen F, Sartor RB, Ozaki M, Jobin C. STAT3 regulates NF-kappaB recruitment to the IL-12p40 promoter in dendritic cells. *Blood* 2005; 105:689-96; PMID:15251981; <https://doi.org/10.1182/blood-2004-04-1309>
29. Pfeiffer IA, Hoyer S, Gerer KF, Voll RE, Knippertz I, Gückel E, Schuler G, Schaft N, Dörrie J. Triggering of NF-kappaB in cytokine-matured human DCs generates superior DCs for T-cell priming in cancer immunotherapy. *Eur J Immunol* 2014; 44:3413-28; PMID:25100611; <https://doi.org/10.1002/eji.201344417>
30. Zee T, Settembre C, Levine RL, Karsenty G. T-cell protein tyrosine phosphatase regulates bone resorption and whole-body insulin sensitivity through its expression in osteoblasts. *Mol Cell Biol* 2012; 32:1080-8; PMID:22252315; <https://doi.org/10.1128/MCB.06279-11>
31. Montalibet J, Skorey K, McKay D, Scapin G, Asante-Appiah E, Kennedy BP. Residues distant from the active site influence protein-tyrosine phosphatase 1B inhibitor binding. *J Biol Chem* 2006; 281:5258-66; PMID:16332678; <https://doi.org/10.1074/jbc.M511546200>
32. Julien SG, Dubé N, Read M, Penney J, Paquet M, Han Y, Kennedy BP, Muller WJ, Tremblay ML. Protein tyrosine phosphatase 1B deficiency or inhibition delays ErbB2-induced mammary tumorigenesis and protects from lung metastasis. *Nat Genet* 2007; 39:338-46; PMID:17259984; <https://doi.org/10.1038/ng1963>
33. Casella CR, Mitchell TC. Putting endotoxin to work for us: monophosphoryl lipid A as a safe and effective vaccine adjuvant. *Cell Mol Life Sci* 2008; 65:3231-40; PMID:18668203; <https://doi.org/10.1007/s00118-008-8228-6>
34. Stagg J, Wu JH, Bouganim N, Galipeau J. Granulocyte-macrophage colony-stimulating factor and interleukin-2 fusion cDNA for cancer gene immunotherapy. *Cancer Res* 2004; 64:8795-9; PMID:15604233; <https://doi.org/10.1158/0008-5472.CAN-04-1776>
35. Frank DA, Mahajan S, Ritz J. Fludarabine-induced immunosuppression is associated with inhibition of STAT1 signaling. *Nat Med* 1999; 5:444-7; PMID:10202937; <https://doi.org/10.1038/7445>
36. Coon ME, Diegel M, Leshinsky N, Klaus SJ. Selective pharmacologic inhibition of murine and human IL-12-dependent Th1 differentiation and IL-12 signaling. *J Immunol* 1999; 163:6567-74; PMID:10586050
37. Schmitt CA, Lowe SW. Bcl-2 mediates chemoresistance in matched pairs of primary E(mu)-myc lymphomas *in vivo*. *Blood Cells Mol Dis* 2001; 27:206-16; <https://doi.org/10.1006/bcmd.2000.0372>
38. Dhodapkar MV, Krasovsky J, Steinman RM, Bhardwaj N. Mature dendritic cells boost functionally superior CD8(+) T-cell in humans without foreign helper epitopes. *J Clin Invest* 2000; 105:R9-R14; PMID:10727452; <https://doi.org/10.1172/JCI9051>
39. Dhodapkar MV, Steinman RM, Sapp M, Desai H, Fossella C, Krasovsky J, Donahoe SM, Dunbar PR, Cerundolo V, Nixon DF. Rapid generation of broad T-cell immunity in humans after a single injection of mature dendritic cells. *J Clin Invest* 1999; 104:173-80; PMID:10411546; <https://doi.org/10.1172/JCI6909>
40. Bussi eres-Marmen S, Vienne V, Gungabeesoon J, Aubry I, P erez-Quintero LA, Tremblay ML. Loss of T-cell protein tyrosine phosphatase in the intestinal epithelium promotes local inflammation by increasing colonic stem cell proliferation. *Cell Mol Immunol* 2017; PMID:28287113; <https://doi.org/10.1038/cmi.2016.72>